IEEE Access
Multidisciplinary | Rapid Review | Open Access Journal

Received October 21, 2019, accepted November 7, 2019, date of publication November 12, 2019,
date of current version December 23, 2019.

Digital Object Identifier 10.1109/ACCESS.2019.2953096

Determination of Fast Corrections for Satellite-Based Augmentation System

SHUAIYONG ZHENG[1], RUI LI[1,2], ZHIGANG HUANG[1], AND BO SHAO[3]
[1]School of Electronic and Information Engineering, Beihang University, Beijing 100191, China
[2]Suzhou Institute, Beihang University, Suzhou 215200, China
[3]20th Research Institute of China Electronics Technology Group Corporation, Xi'an 710000, China

Corresponding author: Zhigang Huang (baahzg@163.com)

This work was supported by the State Key Laboratory of Geo-Information Engineering of China under Grant SKLGIE2018-Z-2-2.

ABSTRACT Fast corrections are the vital parameters of satellite-based augmentation system, mitigating the rapidly changing errors of satellite clock. It is necessary to develop a feasible method to determine fast corrections because the rapidly changing errors of satellite clock badly affect the service performance. For such a purpose, a user equivalent range error-based method is proposed to determine fast corrections in this paper. Firstly, a generation process of satellite corrections is given for the control segment of satellite-based augmentation system. In this process, long-term corrections are generated first. Once the slowly varying errors of satellite ephemeris and clock are eliminated by long-term corrections, a user equivalent range error-based method is developed to solve fast corrections. Finally, the performance of the proposed method is analyzed in signal-in-space domain and position domain. Results demonstrate that compared with WAAS method, the accuracy of signal-in-space is improved by over 25.74% and the integrity bounding rate in pseudorange domain is improved by 4.23%.

INDEX TERMS Satellite-based augmentation system, long-term corrections, fast corrections, Markov process, Kalman filter.

I. INTRODUCTION

Nowdays, Global Navigation Satellite System (GNSS) like GPS has been widely applied to many kinds of vehicles such as cars, trains [1], UAVs [2], and aircrafts [3]. As a representative, the civil aircrafts need pretty high requirements in the aspects of accuracy, integrity, continuity, and availability which is listed in Table 1. The requirements are employed to guarantee flight safety from enroute throughout precision approach, which makes Satellite-Based Augmentation System (SBAS) come into being. SBAS is a well-known augmentation to GNSS that calculates GNSS differential corrections, integrity information, and ranging signals on the ground, and broadcasts augmentation messages to GPS/SBAS users through SBAS satellites (GEOs or IGSOs) [4]–[7].

SBAS can be divided into Single Frequency (SF) SBAS and Dual-Frequency Multi-Constellation (DFMC) SBAS. Even though some SFSBAS like Wide Area augmentation System (WAAS) can provide service for many countries, DFMC SBAS is still under the discussion of standards and can not provide service now [8]. Before the operation of DFMC SBAS, it is meaningful to discuss the technology of control segment for SFSBAS such as Chinese BeiDou SBAS (BDSBAS) and Russian System of Differential Correction and Monitoring (SDCM).

As the key technology of SBAS control segment, satellite ephemeris and clock algorithms have been paid attention for a long time. Before the design and construction of the first SBAS (WAAS), there are some references about the satellite ephemeris and clock algorithms of Wide Area Differential Global Positioning System (WADGPS). As described in the book [7], three dimensional satellite orbit errors and satellite clock errors are all modeled by 1st-order Markov process and satellite ephemeris and clock errors are solved by batch least squares technique simultaneously [9], [10]. Without the consideration of bandwidth, both satellite ephemeris errors and clock errors were taken as fast corrections. In 1996, Enge *et al* put forward a weighted minimum norm method to determine the satellite ephemeris errors and clock errors for wide area augmentation of GPS [11]. Enge gave the message format of long-term corrections and fast corrections for WAAS and did not solve those corrections.

The associate editor coordinating the review of this manuscript and approving it for publication was Lubin Chang.

TABLE 1. ICAO GNSS requirements for different phases of flight [4] (APCH, H and V denote approach, horizontal and vertical, respectively).

Typical operation	Accuracy (H,V)	Integrity probability		Continuity	Availability
		Integrity probability	Alert limit (H,V)		
NPA	220m,–	$1\text{-}1\times10^{-7}$/h	556m,–	$1\text{-}10^{-4}$ – $1\text{-}10^{-8}$/h	0.99 - 0.99999
APV-I	16m,20m	$1\text{-}2\times10^{-7}$/APCH	40m,50m	$1\text{-}8\times10^{-6}$/15s	0.99 - 0.99999
LPV	16m,20m	$1\text{-}2\times10^{-7}$/APCH	40m,50m	$1\text{-}8\times10^{-6}$/15s	0.99 - 0.99999
LPV200	16m,4m	$1\text{-}2\times10^{-7}$/APCH	40m,35m	$1\text{-}8\times10^{-6}$/15s	0.99 - 0.99999
APV-II	16m,8m	$1\text{-}2\times10^{-7}$/APCH	40m,20m	$1\text{-}8\times10^{-6}$/15s	0.99 - 0.99999
CAT-I	16m,4-6m	$1\text{-}2\times10^{-7}$/APCH	40m,10-15m	$1\text{-}8\times10^{-6}$/15s	0.99 - 0.99999

Typically, Tsai from Stanford University utilized a double integrator model and a 2nd-order Markov process to determine satellite ephemeris and clock errors for WADGPS in 1999, respectively [12]. The clock errors in Tsai's research primarily came from Selective Availability (SA). With the technology development of GPS, the position accuracy of GPS can be improved greatly by differential technique. Therefore, SA was canceled in May 2000. In 2012, Grewal conducted a research on orbit determination with Kalman filters for space-based augmentation of GNSS where Grewal set the state of fast clock bias as zero because SA was discontinued [13]. In the same year, without distinguishing between long-term corrections and fast corrections, Shao determined the clock error by a Fourier series-based method after he determined the ephemeris error by a Hill difference equation-based method for SBAS [14], [15]. In 2018, Chen constructed constant turn model and Singer model for satellite ephemeris and clock errors and determined the long-term corrections for DFMC SBAS without the consideration of fast corrections [16], [17].

In a word, WADGPS (or GNSS) is developed for all kinds of applications and the existing satellite ephemeris and clock algorithms for WADGPS aim at the improvement of position accuracy. The integrity of GNSS in pseudorange domain or position domain is not the most important indicator. However, SBAS is developed for civil aviation whose certified users are all safety-of-life users, and the existing satellite ephemeris and clock algorithms for SBAS emphasize the integrity in pseudorange domain and position domain. The position accuracy of GNSS is fit for SBAS users, and SBAS pays more attention to integrity (or safety) than accuracy. To ensure the integrity of SBAS, the satellite corrections are conservative and hence the accuracy of signal-in-space of SBAS is lower than that of GNSS [17]. The problem is how to improve the accuracy of signal-in-space for SBAS without the integrity bounding rate reduced which motivates the authors to develop a feasible method to determine long-term corrections and fast corrections.

In this paper, a user equivalent range error-based (UERE-based) method is developed to determine fast corrections. Firstly, synchronized pseudorange residuals are generated after data preprocessing, and synchronized pseudorange residuals are used to solve long-term corrections. Secondly, UEREs are obtained after synchronized pseudorange residuals are corrected by long-term corrections. Thirdly, UEREs are classified by ring model, and input to least squares estimator, Kalman filter estimator and Sage adaptive filter estimator. Subsequently, fast corrections can be determined after quantified and broadcast. Finally, the performance of the proposed method is compared with that of WAAS in signal-in-space domain and position domain. Results demonstrate that the accuracy the signal-in-space of SBAS is improved by 25.74% and simultaneously the integrity bound rate is improved by 4.23%. Overall, the main contributions of this paper are an algorithm of long-term corrections, an algorithm of fast corrections, and an indicator named tightness to describe the relationship between satellite corrections and integrity information.

This paper is organised as follows: Section 2 describes preliminaries and problem formulation. Section 3 introduces determination of SBAS satellite corrections. Section 4 presents results and analysis. Finally, Section 5 concludes the research with a short summary.

II. PRELIMINARIES AND PROBLEM FORMULATION

A. PRELIMINARIES

SBAS is a safety critical system consisting of a space segment and a ground network to support air navigation from enroute through precision approach. The ground network is composed of monitor stations, master stations, navigation earth station and so forth. Monitor stations are widely dispersed standalone stations that receive and process signals from the GNSS and SBAS satellites. The monitor stations forward their data to master stations, namely, central processing facilities. The master stations process the raw data to determine differential corrections and integrity for each monitored satellites. All those data is packed into SBAS messages, which are sent to navigation earth stations [6], [7].

The architecture of SBAS control segment is illustrated in Fig. 1. As shown in Fig. 1, monitor stations receive and process signals from GNSS and SBAS satellites, and forward those observation data to master stations. Master stations

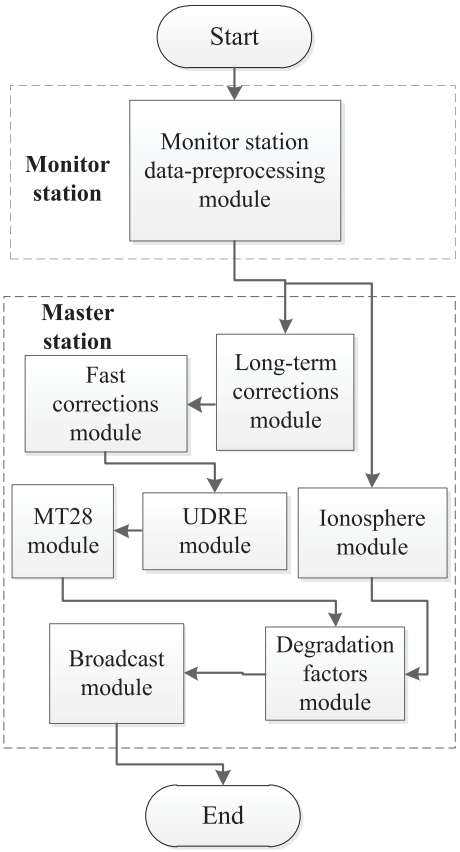

FIGURE 1. Flow chart of SBAS control segment.

process raw data to determine differential corrections and integrity information for each monitored satellite.

More specifically, monitor stations collect dual frequency carrier and code pseudorange. With dual frequency carrier, cycle slip detection and repair is performed by high order difference method [18]. With IFree filter, dual frequency carrier is used to smooth dual frequency code pseudorange and subsequently, ionospheric delay is removed [19], [20]. Meteorological parameters are utilized to compute tropospheric delay [6]. Geometric range can be calculated by broadcast ephemeris and monitor station location. Then, Chi square test is adopted to detect the outliers of monitor stations which ensure the efficiency of time synchronization of monitor stations. Common view time transfer is used to estimate the clock offset of monitor station and synchronized pseudorange residuals. Then, satellite data monitoring is carried out to ensure the quality of synchronized pseudorange residuals. Finally, monitor stations forward their output to master stations.

As for master stations, they consist of long-term corrections module, fast corrections module, User Differential Range Error (UDRE) module, Message Type 28 (MT28) module, ionosphere module, degradation factors module and broadcast module. Master stations make use of data from monitor stations to generate differential corrections and integrity parameters for each monitored satellite. All those

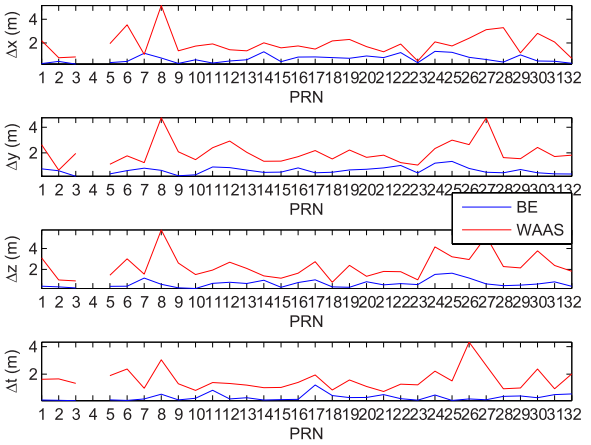

FIGURE 2. Signal-in-space correction errors for WAAS (Note that satellite PRN4 is out of operation).

data is packaged into SBAS messages, which are sent to navigation earth stations.

In short, master stations utilize data from monitor stations to determine long-term corrections and subsequently, use synchronized pseudorange residuals revised by long-term corrections to deduce fast corrections.

B. PROBLEM FORMULATION

In this section, the authors will present a detailed formulation of the problem to improve the accuracy of signal-in-space for SBAS. The signal-in-space correction errors are defined as:

$$\begin{bmatrix} \Delta x \\ \Delta y \\ \Delta z \\ \Delta t \end{bmatrix} = \begin{bmatrix} x \\ y \\ z \\ t \end{bmatrix}_{SBAS} - \begin{bmatrix} x \\ y \\ z \\ t \end{bmatrix}_{PE} \tag{1}$$

where the two vectors with subscripts SBAS and PE are calculated by SBAS messages and precise ephemeris, respectively.

To describe the problem, the source data of the precise ephemeris for antenna phase center is collected from the website of National Geospatial-Intelligence Agency and used as the ground truth to calculate the accuracy of signal-in-space for WAAS first. Then, satellite position and clock offset for WAAS can be determined after long-term corrections and fast corrections are used to revise the satellite position and clock offset from GPS broadcast ephemeris. Finally, the accuracy of signal-in-space on January 1, 2016 for WAAS is calculated and shown in Fig. 2 As shown in Fig. 2, to ensure the integrity of SBAS, the accuracy of signal-in-space of WAAS is more conservative and hence lower than that of GPS.

The problem under consideration is how to improve the accuracy of signal-in-space for SBAS under the prerequisite that the integrity bounding rate between UDRE and signal-in-space correction errors is not reduced. This problem is different from precise orbit determination and precise timing which only emphasize the accuracy of signal-in-space. As for SBAS, it emphasize the integrity in pseudorange domain

and position domain. SBAS pays more attention to integrity (or safety) than accuracy. The objective of this paper is to develop a pseudorange-based method to estimate long-term corrections and fast corrections with the performance of the accuracy of signal-in-space and integrity bounding rate improved.

III. DETERMINATION OF SBAS SATELLITE CORRECTIONS

In this section, the algorithms of long-term corrections and fast corrections algorithms are introduced. Long-term corrections are used for eliminating the slowly varying errors of satellite ephemeris and clock, and fast corrections are used for revising the rapid errors mainly from satellite clock. Fast corrections are determined by pseudorange residuals after the slowly varying errors of satellite clock are removed by long-term corrections. There are two parts in this section: algorithm of long-term corrections and algorithm of fast corrections. After long-term corrections are applied to revising pseudorange residuals, UEREs are classified by ring model. Weighted least squares method is adopted to produce the estimation of the rapidly changing errors which is taken as the observation of Kalman filter. Then, a 2nd-order Gauss Markov process-based model is developed to deduce the state equation of Kalman filter and Sage adaptive filter. After the two filters, the estimation of fast corrections is quantified and broadcast within their maximum update interval.

A. ALGORITHM OF LONG-TERM CORRECTIONS

As is known to all, GNSS ephemeris broadcast by the satellites on orbit provides a so-called source data for computing satellite positions and satellite clock offset. Because of the limitations of the GNSS control segment's ability to predict the satellite ephemeris and clock offset [7], these reported positions and clock offset are in error. Because of complex celestial perturbation, occasionally, the ephemeris can not be predicted by dynamic method preciously. Because the satellite clock errors are affected by their physical characteristics and complex space electromagnetic phenomena, their motion will be disturbed abnormally and satellite clock offset can not be predicted accurately. Although those errors varies slowly, they need to be corrected to satisfy the requirements of SBAS. The long-term corrections are defined to mitigate the slowly varying errors of satellite due to the atmospheric and long term satellite clock and ephemeris errors. In this section, the algorithm of long-term corrections will be introduced below.

When the elevation angle from monitor station to satellite is small, the observation quality of pseudorange residuals is poor. To address this problem, prior information is induced to minimum variance estimator to improve the estimation performance [21], [22]. Additionally, the number of monitor stations in view of satellite changes dramatically, which will lead to the step slip of the output of minimum variance estimator. Consequently, the satellite ephemeris and clock errors output by minimum variance estimator are still greatly sensitive to the geometry of monitor stations, and those estimated values are so noisy that occasionally the estimated results may exceed the range of SBAS messages. To overcome the deficiency of minimum variance estimator, the output of minimum variance estimator is considered as the observation of Kalman filter to correct the Kalman prediction value, and simultaneously the output of minimum variance estimator is smoothed by Kalman filter estimator.

Let $\boldsymbol{p}, \boldsymbol{v}, \boldsymbol{a}, \boldsymbol{\omega}$ be satellite position, velocity, acceleration and angular velocity in Earth-Centered Inertial (ECI) coordinate frame, respectively. Then, by the Poisson's formula [23]

$$\dot{\boldsymbol{\xi}} = \boldsymbol{\omega} \times \boldsymbol{\xi}. \tag{2}$$

Let $\boldsymbol{\xi} = \boldsymbol{v}/v$,we have

$$\dot{\boldsymbol{v}} = \frac{\boldsymbol{v} \cdot \dot{\boldsymbol{v}}}{v^2}\boldsymbol{v} + \boldsymbol{\omega} \times \boldsymbol{v} \tag{3}$$

Furthermore, its equivalent is given by

$$\boldsymbol{\omega} = \frac{\boldsymbol{\omega} \cdot \boldsymbol{v}}{v^2}\boldsymbol{v} + \frac{\boldsymbol{v} \times \boldsymbol{a}}{v^2} \tag{4}$$

As for GNSS satellites, for simplicity, $\boldsymbol{v}$ and $\boldsymbol{a}$ are in a plane orthogonal to $\boldsymbol{\omega}$. Obviously, $\boldsymbol{\omega} \cdot \boldsymbol{v} = 0$. Then, it is clear from formula (4) that the angular velocity is given by

$$\boldsymbol{\omega} = \frac{\boldsymbol{v} \times \boldsymbol{a}}{v^2} \tag{5}$$

In a short time, the velocity $\boldsymbol{v}$ of a GNSS satellite can be taken as a constant speed (i.e., $\dot{\boldsymbol{v}} = 0$). Apparently, $\boldsymbol{a} \cdot \boldsymbol{v} = 0$. It is clear from formula (3) that

$$\boldsymbol{a} = \boldsymbol{\omega} \times \boldsymbol{v} \tag{6}$$

we have the following formula by differentiating formula (6):

$$\dot{\boldsymbol{a}} = -\omega^2 \boldsymbol{v} \tag{7}$$

Therefore, the motion of GNSS satellites can be modeled by a 2nd-order Markov process.

Moreover, satellite clock offset can be modeled by [24]

$$\delta t = a_{f0} + a_{f1}t + \frac{1}{2}a_{f2}t^2 + \varepsilon\,(t) \tag{8}$$

From formula (8), it is clear that satellite clock offset is divided into two parts: deterministic component and random component. The deterministic component can be computed by the quadratic polynomial and its coefficients are clock corrections packed into GNSS navigation message [24], [25]. The random component consists of slow-varying errors and fast-varying errors, which are corrected by long-term corrections and fast corrections, respectively. In this section, slow-varying errors will by modeled next.

It is clear from formula (8) that clock corrections are used to revise the remaining item $\varepsilon\,(t)$, that is, acceleration of clock offset. Given a small τ, a typical representative model of the correlation function $r\,(\tau)$ associated with the acceleration of satellite clock offset is [26], [27]

$$r\,(\tau) = E\,[a\,(t)\,a\,(t+\tau)] = \sigma_m^2 e^{-\alpha|\tau|}, \quad \alpha \geq 0 \tag{9}$$

where σ_m^2 is the variance of satellite clock offset acceleration and α denotes the reciprocal of the acceleration time constant. For example,$\alpha \approx 0.05$ for an evasive maneuver since the reference clocks for GNSS use a combination of high-quality temperature controlled crystal oscillators (TCXO) and atomic clocks based on hyperfine quantum state transitions of atoms, e.g., in rubidium or cesium vapor, [13]. The clock acceleration a(t) can be expressed in terms of Gaussian noise [26], [27] utilizing the correlation function $r(\tau)$. The Laplace transform of the correlation function can be written in 's' domain as follows:

$$R(s) = \frac{-2\alpha\sigma_m^2}{(s-\alpha)(s+\alpha)} = H(s)H(-s)W(s) \tag{10}$$

where

$$H(s) = \frac{1}{s+\alpha} \tag{11}$$

$$W(s) = 2\alpha\sigma_m^2 \tag{12}$$

The functions H(s) and W(s) denote the Laplace transform of the whitening filter for the remaining item of clock offset acceleration and the white noise that drives $a(t)$, respectively. Then, we can obtain the following equation:

$$\dot{a}(t) = -\alpha a(t) \tag{13}$$

In summary, satellite ephemeris and clock offset are modeled by a 2nd-order Markov process and a 1st-order Markov process, respectively. The motion of GNSS satellites can be expressed by [26], [28]–[33]:

$$\dot{\boldsymbol{a_p}} = -\omega^2 \boldsymbol{v} + \boldsymbol{w} \tag{14}$$

where $\boldsymbol{w}$ is a white noise vector, and $\boldsymbol{v}, \boldsymbol{a_p}, \omega$ denote the velocity, acceleration and angular velocity of a specific satellite, respectively. The acceleration of satellite clock offset a_c can be given by [27]:

$$\dot{a}_c(t) = -\alpha a_c(t) + w(t) \tag{15}$$

which is the 1st-order stationary Markov process with a zero-mean [34], [35]. The parameter w is a white noise, and α denote the time constant of this Markov process.

The observation equations are given by formula (16) [16]. In formula (16), $\boldsymbol{X}_{ap}, \boldsymbol{Z}_{PR}, \boldsymbol{X}_{brdc}$ denote prior information, synchronized pseudorange residuals and the vector of satellite position and clock offset.

$$\boldsymbol{Z}(k) = \boldsymbol{R}_{ECEF}^{ECI}\left(\boldsymbol{X}_{ap} + \boldsymbol{\Lambda}\boldsymbol{H}^T\left(\boldsymbol{H}\boldsymbol{\Lambda}\boldsymbol{H}^T + \boldsymbol{R}\right)^{-1} \times \left(\boldsymbol{Z}_{PR} - \boldsymbol{H}\boldsymbol{X}_{ap}\right) + \boldsymbol{X}_{brdc}\right) + \boldsymbol{v}(k) \tag{16}$$

The observation noise matrix is given by

$$\boldsymbol{R}_{\boldsymbol{v}} = \boldsymbol{R}_{ECEF}^{ECI}\begin{bmatrix} \boldsymbol{P}_{1,1} & \boldsymbol{P}_{1,2} & \boldsymbol{P}_{1,3} & 0 \\ \boldsymbol{P}_{2,1} & \boldsymbol{P}_{2,2} & \boldsymbol{P}_{2,3} & 0 \\ \boldsymbol{P}_{3,1} & \boldsymbol{P}_{3,2} & \boldsymbol{P}_{3,3} & 0 \\ 0 & 0 & 0 & \boldsymbol{P}_{4,4} \end{bmatrix}\left(\boldsymbol{R}_{ECEF}^{ECI}\right)^T \tag{17}$$

where $\boldsymbol{R}_{ECEF}^{ECI}$ denotes the rotation matrix from frame ECEF to frame ECI and $\boldsymbol{P}_{i,i}$ denotes the element of $\boldsymbol{P}_{MV}$:

$$\boldsymbol{P}_{MV} = \boldsymbol{\Lambda} - \boldsymbol{\Lambda}\boldsymbol{H}^T\left(\boldsymbol{H}\boldsymbol{\Lambda}\boldsymbol{H}^T + \boldsymbol{R}\right)^{-1}\boldsymbol{H}\boldsymbol{\Lambda} \tag{18}$$

where $\boldsymbol{R}, \boldsymbol{\Lambda}$ denote the covariance of the pseudorange residual vector $\boldsymbol{Z}_{PR}$ and the priori information vector $\boldsymbol{X}_{ap}$, respectively.

Let Kalman filter state

$$\boldsymbol{X} = \begin{bmatrix} x & \dot{x} & \ddot{x} & y & \dot{y} & \ddot{y} & z & \dot{z} & \ddot{z} & t & \dot{t} & \ddot{t} \end{bmatrix}^T \tag{19}$$

where (x,y,z) and t denote the position and clock offset of a specific satellite. Let observation vector

$$\boldsymbol{Z} = \begin{bmatrix} x & y & z & t \end{bmatrix}^T \tag{20}$$

According to formulas (14), (15) and (16), the Kalman filter for long-term corrections is constructed as follows [16]:

$$\begin{cases} \boldsymbol{X}(k) = \boldsymbol{\Phi}(k)\boldsymbol{X}(k-1) + \boldsymbol{w}(k-1) \\ \boldsymbol{Z}(k) = \boldsymbol{H}\boldsymbol{X}(k) + \boldsymbol{v}(k) \end{cases} \tag{21}$$

where

$$\boldsymbol{H} = \begin{bmatrix} 1 & 0 & 0 & 0 & 0 & 0 & 0 & 0 & 0 & 0 & 0 & 0 \\ 0 & 0 & 0 & 1 & 0 & 0 & 0 & 0 & 0 & 0 & 0 & 0 \\ 0 & 0 & 0 & 0 & 0 & 0 & 1 & 0 & 0 & 0 & 0 & 0 \\ 0 & 0 & 0 & 0 & 0 & 0 & 0 & 0 & 0 & 1 & 0 & 0 \end{bmatrix} \tag{22}$$

The propagator matrix is derived by

$$\boldsymbol{\Phi} = \begin{bmatrix} \boldsymbol{\Phi}_x & \boldsymbol{0} & \boldsymbol{0} & \boldsymbol{0} \\ \boldsymbol{0} & \boldsymbol{\Phi}_y & \boldsymbol{0} & \boldsymbol{0} \\ \boldsymbol{0} & \boldsymbol{0} & \boldsymbol{\Phi}_z & \boldsymbol{0} \\ \boldsymbol{0} & \boldsymbol{0} & \boldsymbol{0} & \boldsymbol{\Phi}_t \end{bmatrix} \tag{23}$$

whose elements are obtained by the following formulas:

$$\boldsymbol{\Phi}_x = \boldsymbol{\Phi}_y = \boldsymbol{\Phi}_z = \begin{bmatrix} 1 & \dfrac{\sin(\omega T)}{\omega} & \dfrac{1-\cos(\omega T)}{\omega^2} \\ 0 & \cos(\omega T) & \dfrac{\sin(\omega T)}{\omega} \\ 0 & -\omega\sin(\omega T) & \cos(\omega T) \end{bmatrix} \tag{24}$$

$$\boldsymbol{\Phi}_t = \begin{bmatrix} 1 & T & T^2/2 \\ 0 & 1 & T \\ 0 & 0 & 1 \end{bmatrix} \tag{25}$$

where ω, T denote the instantaneous angular velocity of a specific satellite and the sampling time of this filter. The system noise matrix is given by

$$\boldsymbol{Q}_w = \begin{bmatrix} \boldsymbol{S}_x\boldsymbol{Q}_p & \boldsymbol{0} & \boldsymbol{0} & \boldsymbol{0} \\ \boldsymbol{0} & \boldsymbol{S}_y\boldsymbol{Q}_p & \boldsymbol{0} & \boldsymbol{0} \\ \boldsymbol{0} & \boldsymbol{0} & \boldsymbol{S}_z\boldsymbol{Q}_p & \boldsymbol{0} \\ \boldsymbol{0} & \boldsymbol{0} & \boldsymbol{0} & \boldsymbol{S}_t\boldsymbol{Q}_t \end{bmatrix} \tag{26}$$

where $\boldsymbol{S}_x, \boldsymbol{S}_y, \boldsymbol{S}_z, \boldsymbol{S}_t$ denote the power spectral density and other variables are obtained by formulas (27) and (28), as shown at the bottom of the next page.

According to the output of Kalman filter and navigation message, the slowly changing errors of satellite ephemeris and clock can be deduced. With the estimation during 240s, long-term satellite corrections can be obtained by least

squares method [16] and then packed into the corresponding message type and broadcast within the maximum update interval [6].

B. ALGORITHM OF FAST CORRECTIONS

Once long-term corrections are determined, user equivalent range errors can be obtained after the slowly varying errors of satellite ephemeris and clock are removed from synchronized pseudorange residuals. Then, user equivalent range errors are used to solve fast corrections. In this section, the concept of satellite clock offset will be introduced first and then a UERE-based method is proposed to estimate the rapidly changing errors of satellite clock and generate fast corrections for SBAS or GNSS satellites.

Generally, satellite clock offset is described by formula (8). The parameter a_{fi}, $(i = 1, 2, 3)$ denotes the parameter of broadcast ephemeris to revise clock offset and $\varepsilon(t)$ denotes the random component of clock offset [24], [25]. It is clear that satellite clock offset is divided into two parts: deterministic component and random component. The deterministic component can be computed by a quadratic polynomial and its coefficients (a_{fi}, $(i = 1, 2, 3)$) are clock corrections packed into GNSS broadcast ephemeris. The random component mainly consists of slowly varying errors and fast varying errors, which are revised by long-term corrections and fast corrections, respectively. It is clear that satellite clock corrections are used to revise the remaining item $\varepsilon(t)$, that is, the error caused by the acceleration of clock offset.

Because of highly stable atomic clock, the error of the satellite clock changes very slowly. In most instances, those errors can be mitigated by long-term corrections well. However, sometimes error of satellite clock varies quickly because of clock dither or artificial interfering such as SA. Those errors need to be eliminated to guarantee the service performance of SBAS. As described above, before 2000 there are some references about fast corrections and the rapidly changing errors mainly come from from SA. The characteristic of SA was analyzed and SA was modelled by 2nd-order Gauss Markov process with a standard deviation of 23 meters in range error and 0.28 m/s in range error rate [36], [37]. The model can improve the accuracy of signal-in-space of GNSS with SA dramatically. This model was adopted by the Radio Technical Commission for Aeronautics (RTCA) for receiver testing purposes and written into the standard RTCA MOPS 229 [6], [12]. After SA was cancelled since 2000, the algorithm of fast corrections for WAAS is still the same. Considering that the performance of the current GNSS satellite clock is getting better and better, the rapidly changing error of satellite clock is much smaller than that of before 2000. It can be found that the broadcast value of fast corrections of satellite PRN8 broadcast by WAAS GEO is small and less than 4m in most cases, illustrated in Fig. 3 where PDF denotes probability distribution function. The 2nd-order Gauss Markov model for SA needs to be adjusted to compute fast corrections of SBAS without SA. More importantly, the accuracy of signal-in-space of WAAS is more conservative and hence lower than that of GPS [17]. The 2nd-order Gauss Markov model for SA can not improve the accuracy of signal-in-space of current WAAS well.

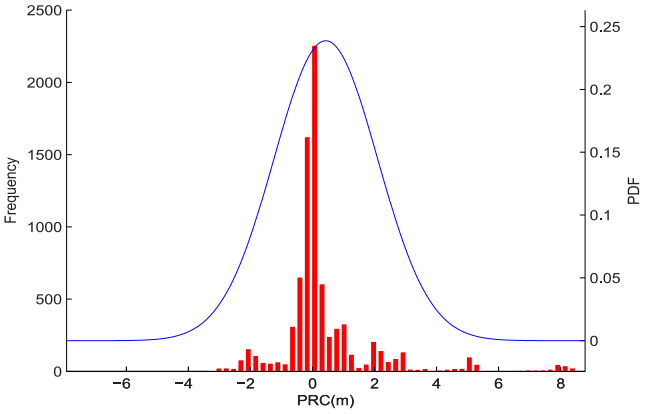

FIGURE 3. Characteristic of WAAS PRN8 fast corrections.

With the consideration of those reasons, a UERE-based method is proposed to solve fast corrections for SBAS. The flow chat of fast correction determination is shown as Fig. 4.

$$\boldsymbol{Q}_p = \begin{bmatrix} \dfrac{6\omega T - 8\sin(\omega T) + \sin(2\omega T)}{4\omega^5} & \dfrac{2\sin^4\left(\dfrac{\omega T}{2}\right)}{\omega^4} & \dfrac{-2\omega T + 4\sin(\omega T) - \sin(2\omega T)}{4\omega^3} \\ \dfrac{2\sin^4\left(\dfrac{\omega T}{2}\right)}{\omega^4} & \dfrac{2\omega T - \sin(2\omega T)}{4\omega^3} & \dfrac{\sin^2(\omega T)}{2\omega^2} \\ \dfrac{-2\omega T + 4\sin(\omega T) - \sin(2\omega T)}{4\omega^3} & \dfrac{\sin^2(\omega T)}{2\omega^2} & \dfrac{2\omega T + \sin(2\omega T)}{4\omega} \end{bmatrix} \tag{27}$$

$$\boldsymbol{Q}_t = \begin{bmatrix} \dfrac{T^5}{20} & \dfrac{T^4}{8} & \dfrac{T^3}{6} \\ \dfrac{T^4}{8} & \dfrac{T^3}{3} & \dfrac{T^2}{2} \\ \dfrac{T^3}{6} & \dfrac{T^2}{2} & T \end{bmatrix} \tag{28}$$

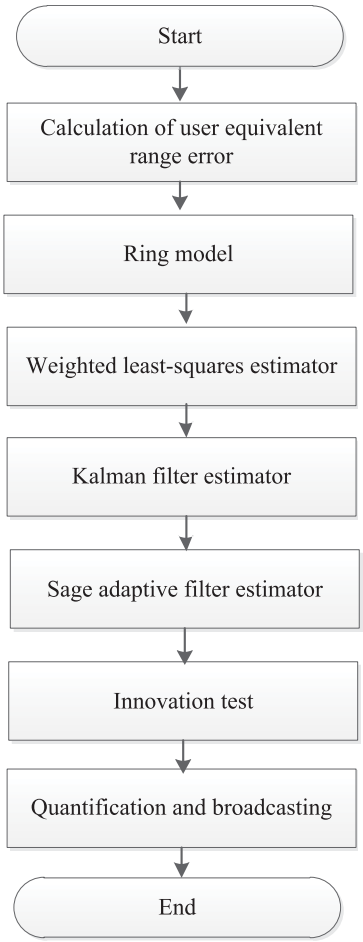

FIGURE 4. Flow chat of fast corrections determination.

As shown in Fig. 4, synchronized pseudorange residuals are revised by long-term corrections to generate UEREs. Then, UEREs are sent to the ring model. When a satellite passes over the network composed of monitor stations, the service volume can be divided into three parts and the Elevation angle (El) form a monitor station to the satellite is shown in Fig. 5. UEREs may be located in each part of this service volume. The UERE with a low elevation angle tends to be corrupted by multipath and receiver thermal noise, and UEREs have to be chosen under some constraints before fast changing errors are estimated. Several cases are considered: (1) When the number of UEREs ($El >= 15°$) is equal or more than 8, only UEREs ($El >= 15°$) are chosen; (2) When the number of UEREs ($El >= 15°$) is less than 8 and the number of UEREs is equal or more than 4, all UEREs are chosen; (3) When the number of UEREs is less than 4, the fast corrections of the satellite are set as null.

Let UEREs after chosen by the above constraints as z_c, and the fast changing errors ΔB can be modeled by:

$$z_c = \boldsymbol{H}_c \Delta B + \boldsymbol{n}_c \tag{29}$$

where $\boldsymbol{n}_c$ a Gaussian noise vector,

$$\boldsymbol{H_c} = \begin{bmatrix} 1 & 0 \end{bmatrix} \tag{30}$$

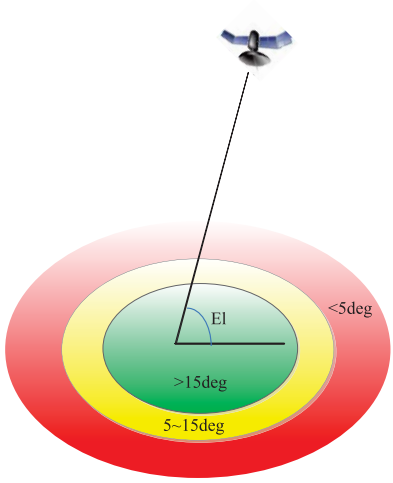

FIGURE 5. Ring model for the service area of a specific satellite.

Rapidly varying errors can be estimated by the weighted least squares estimator with the square of elevation angle from monitor station to satellite as the weight $\boldsymbol{W}_{ci} = El_i^2$:

$$\begin{aligned} \Delta B_c^k &= \left(\boldsymbol{H}_c^T \boldsymbol{W}_c \boldsymbol{H}_c\right)^{-1} \boldsymbol{H}_c^T \boldsymbol{W}_c \boldsymbol{z}_c \\ P_c^k &= \left(\boldsymbol{H}_c^T \boldsymbol{W}_c \boldsymbol{H}_c\right)^{-1} \end{aligned} \tag{31}$$

Since the results of weighted least squares estimator are sensitive to the geometric distribution of monitor stations in view of a specific satellite. Consequently, the results of weighted least squares estimator are taken as the observation of Kalman filter and the prediction estimation of Kalman filter is used to smooth the output of weighted least squares estimator.

As analysed above, a 2nd-order Gauss Markov process is chosen to model the fast changing errors e_c of satellite clock for SBAS:

$$\ddot{e}_c + 2\beta\omega_0 \dot{e}_c + \omega_0^2 e_c = c\omega \tag{32}$$

where $c^2 = 0.002585$, ω_0, ω, β denote the natural frequency, the Gaussian noise with unity power spectral density and the damping ratio, respectively. After this expression (32) is discretized, the state equation of Kalman filter with the state set as $\boldsymbol{X} = \begin{bmatrix} \Delta B^k & \Delta \dot{B}^k \end{bmatrix}^T$ is obtained:

$$\boldsymbol{X}_k = \boldsymbol{\Phi} \boldsymbol{X}_{k-1} + \boldsymbol{\Gamma} \boldsymbol{w}_{k-1} \tag{33}$$

where $\boldsymbol{w}$ denotes a Gaussian noise vector, and other variables can be deduced by formulas (34),(35),(36),(37) and (38), as shown at the bottom of the next page.

$$\boldsymbol{\Gamma} = \begin{bmatrix} \boldsymbol{\Gamma}_{11} & \boldsymbol{\Gamma}_{12} \\ \boldsymbol{\Gamma}_{21} & \boldsymbol{\Gamma}_{22} \end{bmatrix} \tag{35}$$

The results of weighted least squares estimator are taken as the observation of Kalman filter. Obviously,

$$z_k = \boldsymbol{H}_{nc} \boldsymbol{X}_k + \boldsymbol{v}_k \tag{39}$$

where $\boldsymbol{v}$ denotes a Gaussian noise vector and $\boldsymbol{H}_{nc}$ denotes the matrix consisting of n (the line number of z_k) line of $\boldsymbol{H}_c$.

Furthermore, classical Kalman filter estimator is well fit for the situations where observation noise and system noise are zero mean white noise with known statistical characteristics. In fact, the rapidly varying error of satellite clock varies dynamically. It is difficult to obtain its statistical characteristics. Specifically, clock dithers occur frequently especially when satellite clock is working abnormally. At this instance, the disturbance of state equation and observation anomalies has a great effect on the results of Kalman filter. Therefore, Sage adaptive filter estimator is adopted to adjust the parameters of Kalman filter.

Sage adaptive filter estimator uses historical information to estimate the covariance matrices of system noise and observation noise at the current epoch so that the covariance matrices are adaptive to the dynamic information and observation. Then, by using classical Kalman filter, Sage adaptive filter estimator gives the optimal value of system state. In detail, the covariance matrices of system noise and observation noise at the current epoch are estimated by the innovation vector or residual vector of the latest epoch. The estimator of Sage adaptive filter can divided into two types: innovation-based adaptive estimator and residual-based adaptive estimator [38], [39]. Let the innovation vector, residual vector and state update vector as $\boldsymbol{V}_{k|k-1}, \boldsymbol{V}_{k|k}, \Delta\boldsymbol{X}_k$ and they can be computed by

$$\begin{aligned} \boldsymbol{V}_{k|k-1} &= \boldsymbol{H}_{nc}\hat{\boldsymbol{X}}_{k|k-1} - \boldsymbol{z}_k \\ \boldsymbol{V}_{k|k} &= \boldsymbol{H}_{nc}\hat{\boldsymbol{X}}_{k|k} - \boldsymbol{z}_k \\ \Delta\boldsymbol{X}_k &= \hat{\boldsymbol{X}}_{k|k} - \hat{\boldsymbol{X}}_{k|k-1} \end{aligned} \tag{40}$$

The covariance matrix of observation noise is updated by

$$\boldsymbol{R}_k = \frac{1}{m}\sum_{j=0}^{m-1} V_{k-j}V_{k-j}^T - \boldsymbol{H}_{nc}\boldsymbol{P}_{k|k}\boldsymbol{H}_{nc}{}^T \tag{41}$$

where $\boldsymbol{P}_{k|k}$ denotes the covariance matrix of the state estimation at epoch k and m denotes the number of the latest epoch to be used in Sage adaptive process. The covariance matrix of system noise is updated by

$$\boldsymbol{Q}_k = \frac{1}{m}\sum_{j=0}^{m-1} \Delta\boldsymbol{X}_{k-j}\Delta\boldsymbol{X}_{k-j}^T \tag{42}$$

According to formula (41) and formula (42), the covariance matrices of system noise and observation noise can be updated by the data of the latest m epoch.

Subsequently, fault detection and isolation [40] is carried out to remove outliers by innovation test which is performed by the inequation [41]:

$$\left|\boldsymbol{z}_k - \boldsymbol{H}_{nc}\hat{\boldsymbol{X}}_k\right| \geq K_3\sqrt{\boldsymbol{H}_{nc}\boldsymbol{P}_{k|k-1}\boldsymbol{H}_{nc}{}^T + \boldsymbol{R}_k} \tag{43}$$

where $K_3, \boldsymbol{R}_k, \boldsymbol{P}_{k|k-1}$ denotes the threshold corresponding to the confidence 99.9%, the covariance matrix of $\boldsymbol{v}_k$ and the covariance matrix of prediction state, respectively. If the estimation of Kalman filter cannot pass this test, this estimation will be taken as outlier and replaced by the prediction value of this Kalman filter.

Finally, the estimation of fast changing errors of satellite clock is quantified, packed into the corresponding message type and broadcast within its maximum update interval [42]–[44].

The above process is summarized as Algorithm 1.

IV. RESULTS AND ANALYSIS

In this section, the results of the proposed method are compared with that of WAAS method, and results and analysis are presented to demonstrate the rationality and effectiveness of the proposed method. Navigation message (or broadcast ephemeris) is collected from the website of International GNSS Service. Priori information comes from the website of

$$\boldsymbol{\Phi} = \begin{bmatrix} e^{-\beta\omega_0 T}\left[\cos\left(\omega_0 T\sqrt{1-\beta^2}\right) + \frac{\beta}{\sqrt{1-\beta^2}}\sin\left(\omega_0 T\sqrt{1-\beta^2}\right)\right] & \frac{1}{\omega_0\sqrt{1-\beta^2}}e^{-\beta\omega_0 T}\sin\left(\omega_0 T\sqrt{1-\beta^2}\right) \\ -\frac{\omega_0}{\sqrt{1-\beta^2}}e^{-\beta\omega_0 T}\sin\left(\omega_0 T\sqrt{1-\beta^2}\right) & e^{-\beta\omega_0 T}\left[\cos\left(\omega_0 T\sqrt{1-\beta^2}\right) - \frac{\beta}{\sqrt{1-\beta^2}}\sin\left(\omega_0 T\sqrt{1-\beta^2}\right)\right] \end{bmatrix} \tag{34}$$

$$\boldsymbol{\Gamma}_{11} = \frac{c^2}{4\beta\omega_0^3}\left[1 - \frac{1}{\sqrt{\left(\sqrt{1-\beta^2}\right)^3}}e^{-2\beta\omega_0 T}\left(1 - \beta^2\cos\left(2\omega_0 T\sqrt{1-\beta^2}\right) + \beta\sqrt{1-\beta^2}\sin\left(2\omega_0 T\sqrt{1-\beta^2}\right)\right)\right] \tag{36}$$

$$\boldsymbol{\Gamma}_{22} = \frac{c^2}{4\beta\omega_0^3}\left[1 - \frac{1}{\sqrt{\left(\sqrt{1-\beta^2}\right)^3}}e^{-2\beta\omega_0 T}\left(1 - \beta^2\cos\left(2\omega_0 T\sqrt{1-\beta^2}\right) - \beta\sqrt{1-\beta^2}\sin\left(2\omega_0 T\sqrt{1-\beta^2}\right)\right)\right] \tag{37}$$

$$\boldsymbol{\Gamma}_{12} = \boldsymbol{\Gamma}_{21} = \frac{c^2}{4\omega_0^2\left(1-\beta^2\right)}e^{-2\beta\omega_0 T}\left(1 - \cos\left(2\omega_0 T\sqrt{1-\beta^2}\right)\right) \tag{38}$$

Algorithm 1 Fast Corrections Determination Based on User Equivalent Range Errors)

Step 1: Receive observation data and navigation message and preprocess to generate synchronized pseudorange $\boldsymbol{Z}_{PR}$ residuals by monitor station data-preprocessing module.

Step 2: According to formulas (16), (18), (21), etc, synchronized pseudorange residuals are used to generate long-term corrections by the subsection of algorithm of long-term corrections.

Step 3: Synchronized pseudorange residuals are corrected by long-term corrections and then the new pseudorange residuals (termed as UEREs) are processed by ring model.

Step 4: The pseudorange residuals processed by ring model are input to least squares estimator in formula (31).

Step 5: The output of least squares estimator is input to Kalman filter estimator in formulas (33) and (39).

Step 6: The parameters of Kalman filter estimator are updated by Sage adaptive filter estimator in formulas (41) and (42), and innovation test is performed by formula (43).

Step 7: Quantify and broadcast fast corrections.

Step 8: End if the mission of fast corrections determination is accomplished. Otherwise, go back to Step 1.

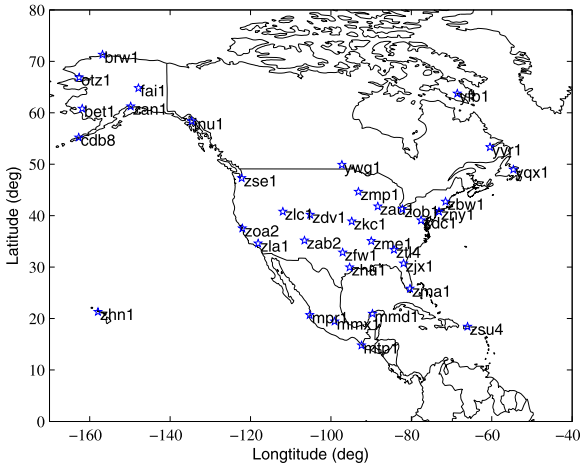

FIGURE 6. Distribution of 36 monitor stations.

National Geospatial-Intelligence Agency. Observation data comes from the website of National Geodetic Survey and the geometry of selected monitor stations is shown in Fig. 6. There are two parts in this section: part A and part B. In part A, signal-in-space domain performance is analyzed in four aspects (analysis of broadcast fast corrections characteristic, signal-in-space correction errors, trend of User Differential Range Error Indicator (UDREI) and integrity bounding to satellite corrections). In part B, position domain performance is analyzed in four aspects of accuracy, integrity, continuity and availability.

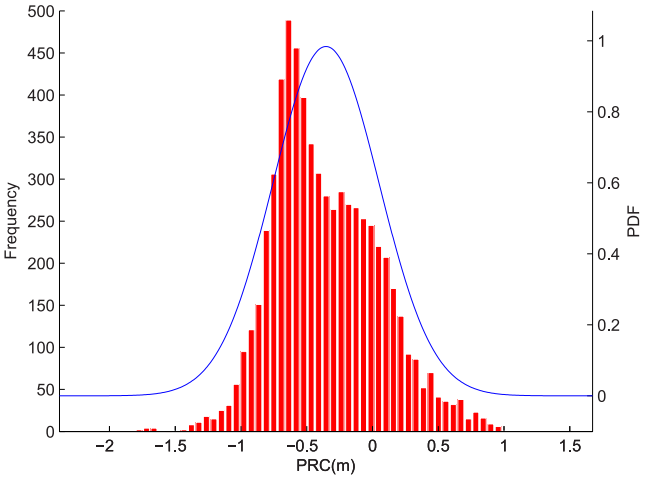

FIGURE 7. Characteristic of PRN8 fast corrections.

A. VALIDATION OF SIGNAL-IN-SPACE DOMAIN PERFORMANCE

To validate the performance of the proposed method, the signal-in-space domain performance is analyzed in the following four aspects.

1). Analysis of broadcast fast corrections characteristic

To analyze broadcast fast corrections characteristic, a normal distribution-based method is adopted to fit the broadcast fast corrections of PRN8 [45], [46], depicted in Fig. 7. The broadcast fast corrections are nearly subject to Gaussian distribution which is consistent with the UERE-based method for fast corrections. An conclusion can be made that the broadcast fast corrections follow Gaussian distribution which suggests the UERE-based method is reasonable to some degree.

2). Signal-in-space correction errors

Define a variable $v_i\,(v = \Delta x, \Delta y, \Delta z, \Delta t; i = 1, 2, 3)$ to indicate the elements of corrections errors defined by formula (1). The variables v_1, v_2, v_3 are computed by the data of Broadcast Ephemeris (BE), the SBAS messages (long-term corrections and fast corrections) generated by the proposed method, and WAAS messages (long-term corrections and fast corrections) of WAAS GEO, respectively. The root mean squares of signal-in-space correction errors with respect to all GPS satellites are shown in Fig. 8.

According to Fig. 8, the signal-in-space errors of the proposed method and broadcast ephemeris method are smaller than that of WAAS method. The accuracy of signal-in-space of the proposed method is more than 18.22% higher than that of broadcast ephemeris method in the three dimensions of orbit while the accuracy of signal-in-space of WAAS method is lower than that of broadcast ephemeris method in those three dimensions. The accuracy of signal-in-space of the proposed method is over 32.03% higher than that of WAAS method in orbit. As for satellite clock, the accuracy of signal-in-space of both the proposed method and WAAS method is lower than that of broadcast ephemeris method. The accuracy of signal-in-space of the proposed method is over 25.74%

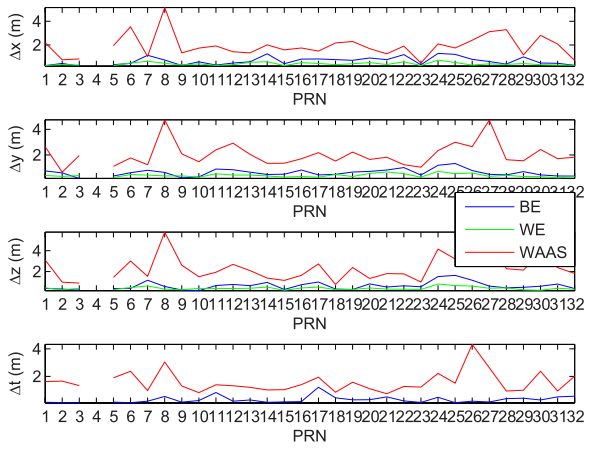

FIGURE 8. Comparison of signal-in-space correction errors between the proposed method and WAAS method (Note that satellite PRN4 is out of operation).

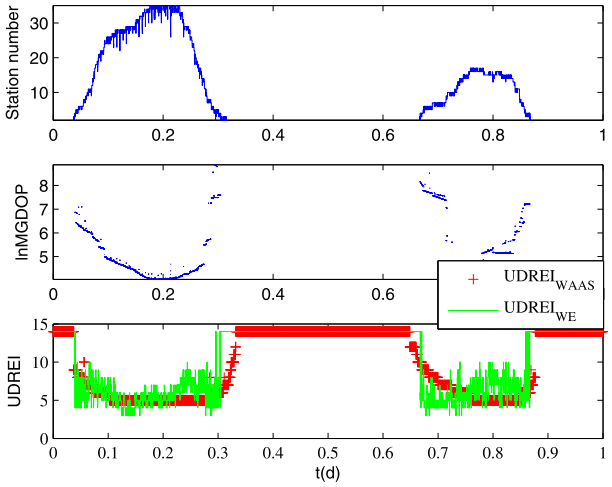

FIGURE 9. Monitor station number in view of satellite PRN8 and UDREI.

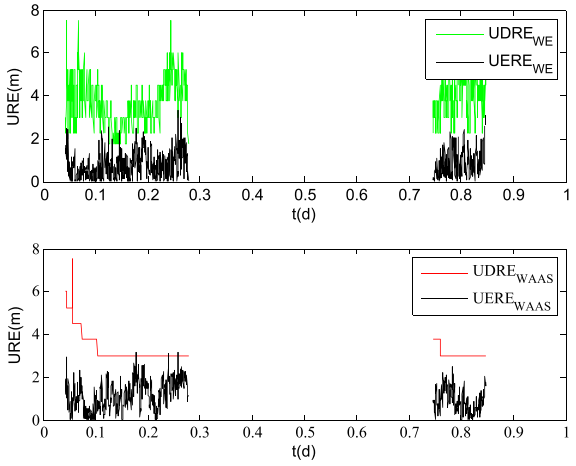

FIGURE 10. Pseudorange correction errors versus UDRE estimates for the user station zfw1.

higher than that of WAAS method in clock. In total, compared with WAAS method, the proposed method can improve the accuracy of signal-in-space by over 25.74%. An conclusion can be drawn that SBAS is designed to ensure the integrity at the expense of accuracy of signal-in-space.

3). Trend of user differential range error indicator

Take satellite PRN8 as an example, the number of monitor stations in view of PRN8 on January 1, 2016 is shown in Fig. 9. The geometry of those monitor stations is quantified by [47]:

$$\ln MGDOP = \ln\left(\sqrt{trace\left[(\boldsymbol{G}^T\boldsymbol{G})^{-1}\right]}\right) \tag{44}$$

where $\boldsymbol{G}$ denotes the geometry matrix whose elements in each line are composed of a unit vector from satellite to monitor station for the first three dimensional and 1 for the fourth dimensional.

From Fig. 9, it can be concluded that the trends of lnMGDOP and the number of monitor station in view of satellite PRN8 go conversely, and the trends of UDREI (or UDRE) and lnMGDOP are identical which is coincident with the concept of satellite motion and integrity monitoring.

4). Integrity bounding to satellite corrections

UDRE (along with MT28) is an error bound on ephemeris and clock corrections of a specific satellite in its service area. Pseudorange residuals corrected by long-term corrections and fast corrections are termed as URE_{flt}. The relationship between UDRE (with respect to the service area of a specific satellite) and URE_{flt} is depicted in Fig. 10.

Furthermore, define a variable

$$\sigma_{flt} = K_3\sigma_{UDRE}\sqrt{\boldsymbol{I}^T\boldsymbol{R}^T\boldsymbol{R}\boldsymbol{I}} \tag{45}$$

where $K_3 = 3.2905$ [15], σ_{UDRE} can be reckoned from the lookup table of UDRE (UDREI), $\boldsymbol{I}$ denotes the unit vector along the user-to-satellite line of sight augmented by 1 for the time component, and $\boldsymbol{R}$ is an upper triangular matrix which can be determined by message type 28 [6], [48], [49]:

$$\boldsymbol{R} = scale\ factor \times \boldsymbol{E} \tag{46}$$

where *scale factor* and $\boldsymbol{E}$ are the parameters in message type 28. The bounding standard σ_{flt} is a equivalent form of UDRE and MT28.

Further, define a parameter named tightness to evaluate the relationship between σ_{flt} and URE_{flt}:

$$\eta = \frac{\sigma_{flt} - \left|URE_{flt}\right|}{\sigma_{flt}} \tag{47}$$

The tightness with respect to the pair the satellite PRN8 and the user station zfw1 is shown in Fig. 11. The tightness for each satellite is shown in Fig. 12. From Figs. 11 and 12, it is clear that the tightness for each satellite computed by the proposed method is similar to that of WAAS method. Compared with WAAS method, the integrity bounding is improved by 4.23% averagely.

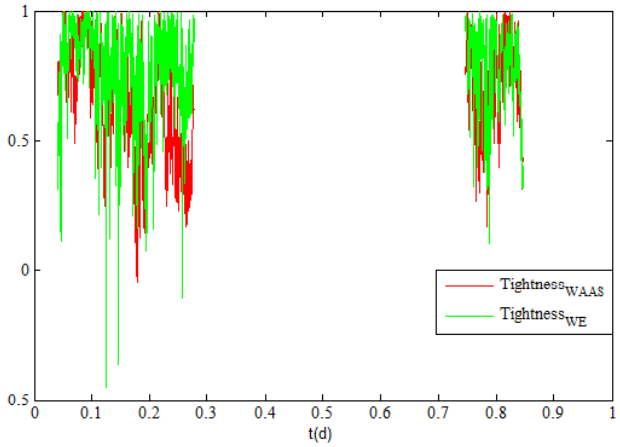

FIGURE 11. Tightness between pseudorange correction errors and error bounds for the user station zfw1.

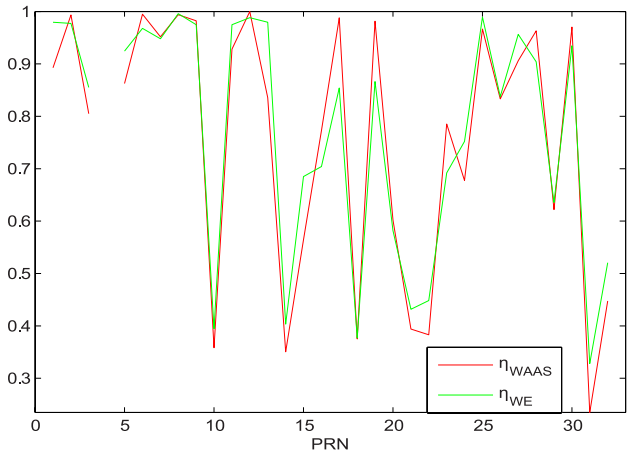

FIGURE 12. Comparison of bound percent of GPS satellites.

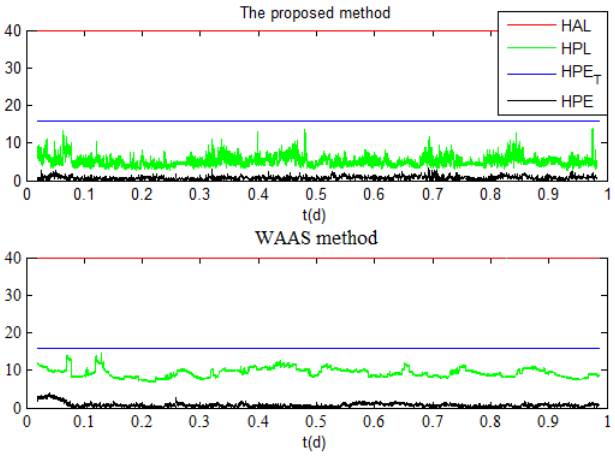

FIGURE 13. Horizontal position results of the user station zfw1 with the proposed method.

B. VALIDATION OF POSITION DOMAIN PERFORMANCE

To analyze the position domain performance, some stations are chosen as users. The position results are shown in Figs. 13 and 14, and Table. 2. In both figures, HPE, HPE_T,

TABLE 2. Service performance of the proposed method and WAAS method (Note: IP denotes integrity probability.)

User	Accuracy	IP	Continuity	Availability
bet1$_{WAAS}$	1.3m,1.4m	1.0000	0.9987	0.9900
bet1$_{WE}$	1.5m,2.2m	1.0000	0.9927	0.9500
mmd1$_{WAAS}$	1.8m,1.8m	1.0000	0.9978	0.9900
mmd1$_{WE}$	1.7m,2.1m	1.0000	0.9988	0.9900
ywg1$_{WAAS}$	1.4m,1.7m	1.0000	1.0000	0.9900
ywg1$_{WE}$	1.7m,1.6m	1.0000	1.0000	0.9800
yqx1$_{WAAS}$	1.4m,1.9m	1.0000	0.9980	0.9900
yqx1$_{WE}$	1.6m,2.5m	1.0000	0.9943	0.9500
zbw1$_{WAAS}$	1.7m,2.2m	1.0000	1.0000	0.9900
zbw1$_{WE}$	1.9m,2.5m	1.0000	0.9989	0.9800
zdv1$_{WAAS}$	1.7m,1.6m	1.0000	1.0000	0.9900
zdv1$_{WE}$	1.9m,1.7m	1.0000	1.0000	0.9800
zan1$_{WAAS}$	1.4m,1.7m	1.0000	1.0000	0.9900
zan1$_{WE}$	1.6m,2.0m	1.0000	0.9995	0.9500
zfw1$_{WAAS}$	2.0m,1.4m	1.0000	1.0000	0.9900
zfw1$_{WE}$	2.0m,1.6m	1.0000	1.0000	0.9800
zau1$_{WAAS}$	1.8m,2.3m	1.0000	1.0000	1.0000
zau1$_{WE}$	1.7m,1.8m	1.0000	1.0000	0.9800

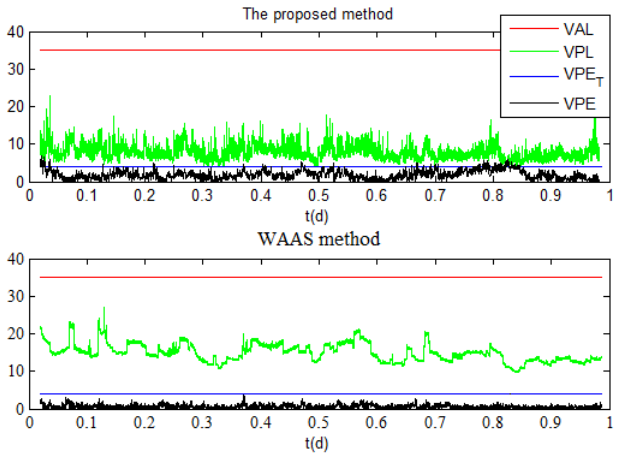

FIGURE 14. Vertical position results of the user station zfw1 with the proposed method.

HPL, HAL, VPE, VPE_T, VPL, VAL denote horizontal position error, the threshold of horizontal position error set by LPV200, horizontal protection level, horizontal alert limit, vertical position error, the threshold of vertical position error set by LPV200, vertical protection level, and vertical alert limit, respectively. HPE_T, VPE_T, HAL, and VAL are set as 16m, 4m, 40m, and 35m, respectively [4].

As shown in Figs. 13 and 14, the results of the proposed method show that VPE<VPE_T in most case and VPE<VPL<VAL in all cases. The position accuracy of the user zfw1 is 2.0m horizontally and 1.6m vertically. The LPV200 availability for the user zfw1 is 98% under the constraints VPE<VPE_T and VPE<VPL<VAL. To further analyze the user performance of the proposed method,

more users are chosen to gather statistics, listed in Table. 2. For those users, the accuracy and integrity of the proposed method are similar to that of WAAS method, and meet the requirements of LPV200 while the continuity and availability are slightly lower than that of WAAS method (or the requirements of LPV200). The accuracy and integrity of the proposed method in position domain are similar to that of WAAS method which can meet the requirements of LPV200 for most North America. In short, results reveal that the proposed method provides satisfactory service performance.

V. CONCLUSIONS AND DISCUSSIONS

In this paper, a user equivalent range error-based method is proposed to estimate the fast corrections for each satellite. The performance of this method is analyzed compared with WAAS method in signal-in-space domain and position domain. The value of fast corrections output by the proposed method is similar to that of WAAS GEO which suggests the correctness and rationality of the proposed method. The main contributions of this paper are an algorithm of long-term corrections, an algorithm of fast corrections, and an indicator named tightness to describe the relationship between satellite corrections and integrity information. The advantages of the proposed method include:

1) The user equivalent range error-based method takes into account multipath and receiver thermal noise for satellite corrections determination and satellite integrity monitoring. A ring model is proposed to process user equivalent range errors in cast that some noise from multipath and receiver interferes the estimation of fast corrections.

2) The user equivalent range error-based concerns the accuracy of signal-in-space and satellite integrity monitoring simultaneously. This paper gives an indicator named tightness to describe the relationship between satellite corrections and satellite integrity which is beneficial for understanding the concept of SBAS. In contrast to WAAS, the proposed method presents a better accuracy of signal-in-space. Results demonstrate that the proposed method can improve the accuracy of signal-in-space and the bounding rate in pseudorange domain by 25.74% and 4.23%, respectively.

3) The user equivalent range error-based method has a high real-time ability. The covariance matrix of Kalman filter for fast corrections is updated by Sage adaptive filter in real time. The covariance matrices of system noise and observation noise can reveal the characteristics of fast changing errors of some satellite in time.

According to results and analysis, the accuracy and integrity of the proposed method in position domain are similar to that of WAAS method which can meet the requirements of LPV200 for most North America. The continuity and availability of the proposed method in position domain are slightly lower than that of WAAS method. To improve the performance of the proposed method, some other issues also need further investigations in the future work. One important issue is that the time synchronization of monitor stations is performed by common view time transfer whose accuracy is limit to the current technology and still not perfect. Since the proposed method is based on user equivalent range errors which are computed from pseudorange residuals removed by the clock error of monitor stations, the optimization of the time synchronization of monitor stations is benefit for improving the precision of user equivalent range errors and hence the precision of fast corrections. Another issue is related to the service availability in position domain. The service availability needs to be improved to satisfy the requirements of LPV200. Availability is an important comprehensive indicator of satellite-based augmentation system which is closely related to the usage time of satellite-based augmentation system for users. Future work will include further research on the time synchronization of monitor stations and the improvement of service availability.

REFERENCES

[1] J. Beugin, "Safety appraisal of GNSS-based localization systems used in train spacing control," *IEEE Access*, vol. 6, pp. 9898–9916, 2018.

[2] Z. Y. Zhao, "A performance evaluation algorithm of stochastic hybrid systems based on fuzzy health degree and its application to quadrotors," *IEEE Access*, vol. 6, pp. 37581–37594, 2018.

[3] B. Chen, D. Gao, and L. Wang, "Research of multi-information integration for the aircraft ground centralized deicing monitoring system based on wireless data transmission," *IEEE Access*, vol. 6, pp. 52460–52470, 2018.

[4] *ICAO SARPS Annex 10: International Standards and Recommended Practices, Aeronautical Telecommunications*, Int. Civil Aviation Org., Montréal, QC, Canada, 2006.

[5] R. A. Fuller, R. Hayward, and J. Christie, "Global augmentation to global positioning system," U.S. Patent 6 531 981, Mar. 2003.

[6] *Minimum Operational Performance Standards for Global Positioning System/Satellite-Based Augmentation System Airborne Equipment*, document RTCA DO-229E, SC-159, 2013.

[7] B. W. Parkinson, *Global Positioning System: Theory and Applications*, vol. 2. Washington, DC, USA: American Institute of Aeronautics and Astronautics, 1996, pp. 81–142.

[8] *Satellite-Based Augmentation System Interoperability Working Group*, SBAS L5 DFMC Interface Control (SBAS L5 DFMC ICD) Revision 3, Noordwijk, The Netherlands, 2016, no. 1, pp. 1–53.

[9] C. Kee, B. W. Parkinson, and P. Axelrad, "Wide area differential GPS," *Navigation*, vol. 38, no. 2, pp. 123–145, 1991.

[10] C. Kee and B. Parkinson, "Algorithms and implementation of wide area differential GPS," in *Proc. ION GPS*, Albuquerque, NM, USA, 1992, pp. 1–5.

[11] P. Enge, "Wide area augmentation of the global positioning system," *Proc. IEEE*, vol. 84, no. 8, pp. 1063–1088, Aug. 1996.

[12] Y. J. Tsai, "Wide area differential operation of the global positioning system: Ephemeris and clock algorithms," Stanford Univ., San Francisco, CA, USA, 1999.

[13] M. S. Grewal, "Space-based augmentation for global navigation satellite systems," *IEEE Trans. Ultrason., Ferroelectr., Freq. Control*, vol. 59, no. 3, pp. 497–503, Mar. 2012.

[14] B. Shao, "Research on integrity key technology of user differential range error for mixed constellation," Beihang Univ., Beijing, China, 2012.

[15] B. Shao, "A user differential range error calculating algorithm based on analytic method," *Chin. J. Aeronaut.*, vol. 24, no. 6, pp. 762–767, 2011.

[16] J. Chen, Z. G. Huang, and R. Li, "Computation of satellite clock-ephemeris corrections using *a priori* knowledge for satellite-based augmentation system," *GPS Solutions*, vol. 21, no. 2, pp. 663–673, 2017.

[17] C. Jie, Z. H. Huang, and R. Li, "Computation of satellite clock-ephemeris augmentation parameters for dual-frequency multi-constellation satellite-based augmentation system," *J. Syst. Eng. Electron.*, vol. 29, no. 6, pp. 1111–1123, 2018.

[18] J. Chen, Z. G. Huang, and R. Li, "Real-time cycle slip detection and repair algorithm for SBAS airborne receiver," in *Proc. China Satell. Navigat. Conf. (CSNC)*, in Lecture Notes in Electrical Engineering, vol. 2. Berlin, Germany: Springer, 2015, pp. 101–112.
[19] P. Y. Hwang, G. A. McGraw, and J. R. Bader, "Enhanced differential GPS carrier-smoothed code processing using dual-frequency measurements," *Navigation*, vol. 46, no. 2, pp. 127–137, 1999.
[20] H. Konno, "Evaluation of two types of dual-frequency differential GPS techniques under anomalous ionosphere conditions," in *Proc. ION NTM*, 2006, pp. 18–20.
[21] T. Kailath, A. H. Sayed, and B. Hassibi, *Linear Estimation*. Upper Saddle River, NJ, USA: Prentice-Hall, 2000.
[22] A. Gelb, *Applied Optimal Estimation*. Cambridge, MA, USA: MIT Press, 1974.
[23] A. Miele, *Flight Mechanics: Theory of Flight Paths*. New York, NY, USA: Dover, 2016.
[24] E. D. Kaplan and C. J. Hegarty, *Understanding GPS Principles and Applications*. Norwood, MA, USA: Artech House, 2006.
[25] G. Xie, *Principles of GPS and Receiver Design*. Beijing, China: House of Electronics Industry, 2009.
[26] X. R. Li and P. V. Jilkov, "Survey of maneuvering target tracking. Part I. Dynamic models," *IEEE Trans. Aerosp. Electron. Syst.*, vol. 39, no. 4, pp. 1333–1364, Oct. 2003.
[27] R. A. Singer, "Estimating optimal tracking filter performance for manned maneuvering targets," *IEEE Trans. Aerosp. Electron. Syst.*, vol. AES-6, no. 4, pp. 473–483, Jul. 1970.
[28] X. R. Li and P. V. Jilkov, "Survey of maneuvering target tracking. Part II: Motion models of ballistic and space targets," *IEEE Trans. Aerosp. Electron. Syst.*, vol. 46, no. 1, pp. 96–119, Jan. 2010.
[29] X. R. Li and P. V. Jilkov, "Survey of maneuvering target tracking. Part V. Multiple-model methods," *IEEE Trans. Aerosp. Electron. Syst.*, vol. 41, no. 4, pp. 1255–1321, Oct. 2005.
[30] X. R. Li and P. V. Jilkov, "Survey of maneuvering target tracking part I: Dynamic models," *Proc. SPIE*, vol. 39, no. 4, pp. 1333–1364, 2003.
[31] X. R. Li and P. V. Jilkov, "Survey of maneuvering target tracking part II: Ballistic target models," *Proc. SPIE*, vol. 4473, no. 63, pp. 559–581, 2001.
[32] X. R. Li and P. V. Jilkov, "Survey of maneuvering target tracking part III: Measurement models," *Proc. SPIE*, vol. 4473, no. 41, pp. 423–447, 2001.
[33] X. R. Li and P. V. Jilkov, "Survey of maneuvering target tracking: Decision-based methods," *Proc. SPIE*, vol. 4728, no. 60, pp. 511–535, 2002.
[34] R. M. Blumenthal and R. K. Getoor, *Markov Processes and Potential Theory*. North Chelmsford, MA, USA: Courier Corporation, 2007.
[35] S. N. Ethier and T. G. Kurtz, *Markov Processes: Characterization and Convergence*. Hoboken, NJ, USA: Wiley, 2009.
[36] G. Matchett, "Stochastic simulation of GPS selective availability," FAA, Washington, DC, USA, Tech. Rep. DTRS-57-83-C-00077, Jun. 1985.
[37] J. Studenny, "Simulation of a second-order Gauss–Markov process," RTCA, Washington, DC, USA, White Paper 148-93/SC159-424, Mar. 1993.
[38] B. D. Anderson and J. B. Moore, *Optimal Filtering*. North Chelmsford, MA, USA: Courier Corporation, 2012.
[39] A. H. Mohamed and K. P. Schwarz, "Adaptive Kalman filtering for INS/GPS," *J. Geodesy*, vol. 73, no. 4, pp. 193–203, 1999.
[40] E. S. Wang, M. Cai, and T. Pang, "A simple and effective GPS receiver autonomous integrity monitoring and fault isolation approach," in *Proc. Int. Conf. IEEE Control Eng. Commun. Technol.*, Dec. 2012, pp. 657–660.
[41] Z. Shuai-Yong, F. Qiang, H. Tereshchenko, W. Ti-Qiang, and Q. Quan, "An initial research on ultra-wideband and inertial measurement unit pose estimation for unmanned aerial vehicle," in *Proc. IEEE Chin. Guid., Navigat. Control Conf. (CGNCC)*, Aug. 2016, pp. 1834–1839.
[42] R. E. Kalman, "A new approach to linear filtering and prediction problems," *J. Basic Eng.*, vol. 82, no. 1, pp. 35–45, 1960.
[43] B. Ristic, S. Arulampalam, and N. Gordon, "Beyond the Kalman filter," *IEEE Aerosp. Electron. Syst. Mag.*, vol. 19, no. 7, pp. 37–38, Oct. 2004.
[44] P. Kim, "Kalman filter for beginners: With MATLAB examples," CreateSpace, Scotts Valley, CA, USA, 2011.
[45] R. Li, "Evaluation of GNSS signal-in-space continuity: A weibull-distribution-based method," *Chin. J. Electron.*, vol. 27, no. 3, pp. 634–640, 2018.
[46] M. S. Hamada, *Bayesian Reliability*. Berlin, Germany: Springer, 2008, pp. 1–120.
[47] J. Chen, "An efficient algorithm for determining the correspondence between DFREI and S DFRE for a dual-frequency multi-constellation satellite-based augmentation system," in *Proc. 8th CSNC*, Shanghai, China, 2017, pp. 109–118.
[48] J. T. Wu and S. Peck, "An analysis of satellite integrity monitoring improvement for WAAS," in *Proc. ION GNSS*, 2002, pp. 756–765.
[49] T. Walter, A. Hansen, and P. Enge, "Message type 28," in *Proc. ION GNSS*, Long Beach, CA, USA, 2001, pp. 522–532.

SHUAIYONG ZHENG was born in 1991. He is currently pursuing the Ph.D. degree in communications and information systems with Beihang University. His research interests cover satellite-based augmentation systems, inertial navigation systems, and ultra wideband systems.

RUI LI was born in 1976. He received the Ph.D. degree from Beihang University, in 2006. He is currently a Senior Engineer with the School of Electronics and Information Engineering, Beihang University. His main interests include RNP and GNSS augmentation technologies in SBAS, GBAS, and ABAS.

ZHIGANG HUANG was born in 1962. He received the Ph.D. degree from Beihang University, in 2004. He is currently a Professor with the School of Electronics and Information Engineering, Beihang University. His research interests include integrity algorithms, and related software for GBAS and SBAS.

BO SHAO was born in 1983. He received the Ph.D. degree from Beihang University, in 2012. He is currently an Engineer with the 20th Research Institute of China Electronics Technology Group Corporation. His research interests include SBAS integrity algorithms and SBAS related software.